International Refereed Journal of Engineering and Science (IRJES)
ISSN (Online) 2319-183X, (Print) 2319-1821
Volume 5, Issue 12 (December 2016), PP.43-54

Adsorption Characteristics of Phosphate on Acid Insoluble Residue Derived From waste iron ore Tailings.

Dr. S. K. Giri
[1]*Lecturer, Department of Chemistry, Seemanta Mahavidyalaya, Jharpokharia Mayurbhanj Orissa, India*

Abstract: Experimental Investigation were carried out to adsorb phosphate from aqueous medium using acid insoluble residue (AIR) as an adsorbent, obtained from waste iron ore tailings (IOT) as the starting materials in this study. Waste IOT contains 55.78% Fe_2O_3, 16.58% SiO_2, and 15.46% Al_2O_3 have been subjected to 1:1 HCl digestion to extract the entire amount of Fe_2O_3 as $FeCl_3$. The AIR was removed as impurities by filtration, with minimum washing using distilled water to make clear $FeCl_3$ solution from impurities (AIR). The AIR contains 0.64% Fe_2O_3, 59.59% SiO_2, and 24.40% Al_2O_3 act as good adsorbent due to presence of high percentage of silica and alumina. Batch adsorption experiments were performed at different operating conditions like: adsorbate concentration, pH, temperature, adsorbent dose and contact time. Maximum adsorption of phosphate was observed upto pH= 6-7, then decreases. The whole process is carried out to maintain pH ~ 6. Pseudo second order kinetics model explain successfully the kinetic data and found to fit the equilibrium data more adequately. Also the thermodynamic parameters such as ΔH^0, ΔS^0 and ΔG^0 were determined. Waste IOT, phosphate adsorb on AIR are characterized by XRD, FTIR spectrophotometer and chemical analysis.
Keywords: Waste IOT; Acid Insoluble Residue; Adsorption; Phosphate.

I. INTRODUCTION

In recent years, environmental pollution is one of the major threats to human life. Among the different types of pollution, waste water stream is one of the major problems due to large amount of water used in our daily life. Waste water containing phosphate is the major source of water pollution. Phosphate is essential for plant growth in soils and has been recognized as one of the main nutrients that controls eutrophication in surface water bodies [1,2]. A continuing elevated level of phosphorus in stagnant water systems stimulates growth of aquatic plants and toxic cyanobacteria. The common forms of phosphorus in waste water are polyphosphates (Polymers of Phosphoric acid), organically bound phosphates, and the most abundant orthophosphates [3]. Large quantities of phosphates are used in many industrial applications with fertilizers being the most important. Other applications include domestic use of detergents containing phosphate formulations as well as excessive fertilizer application to agricultural lands. Phosphorus content of effluents or streams that discharge directly into lakes and dams is regulated by national and international water standard authorities with maximum limits ranging from 0.1 to 2.0 mg/L as P, and may established at 1.0 mg/L [3].

A study on water and waste water quality in Blantye, Malawi, revealed phosphate concentrations ranging from 0.63 to 5.50 mg/L in some streams and effluent from some waste water treatment plants [4]. Phosphorus is a Group 5A element having pentalvalent oxoaniond structure and chemical reactivity. Many laboratory experiments have demonstrated that these oxoanions have similar adsorption behavior on solid surfaces [5-8]. This indicates need for phosphate removal during waste water treatment in an effort to present eutrophication of stagnant water bodies onto which the effluent is discharged. Conventional methods for phosphorus removed from waste water include physical [9,10], chemical [11], biological [12] and crystallization methods [13]. Also flotation has been used to remove orthophosphates from solutions [14]. Chemical removal techniques are the most effective and well-establishe methods, including phosphate precipitation with calcium, aluminum and iron salt [15-17]. However, the cost associated with the use of metal salts may hinder the widespread application. Besides, the product of chemical immobilization is metal phosphate sludge, which is disposed with relatively high phosphorus content, as the recovery of phosphorus from sludge is very difficult. Consequently, there has been growing interest in search for low cost materials can be used for phosphate removal during waste water treatment.

The aim of this article is to perform an adsorption of phosphate on AIR obtained from waste IOT. Waste IOT have been subjected to 1:1 HCl digestion to extract the entire amount of Fe_2O_3 as $FeCL_3$. The AIR was removed by filtration, with minimum washing using distilled water to make clear $FeCl_3$ solution from impurities (AIR). This AIR contains good percentage of silica and alumina and has been used as adsorbent for removal of phosphate from contaminated water. The study is done at different concentration of phosphate, pH, temperature, adsorbent doses and contact time. The whole process is carried out to maintain pH ~ 6. Pseudo second order kinetics model explain successfully the kinetic data. Also the thermodynamic parameters such as

ΔH^0, ΔS^0 and ΔG^0 were determined. Waste IOT and phosphate adsorb on AIR are characterized by XRD, FTIR spectrophotometer and chemical analysis.

II. EXPERIMENTAL

2.1. Materials

Waste IOT was collected from outside of iron ore industries (Joda-Barbil, Orissa, India) as one of the staring materials to produced AIR, Conc. HCl (Merck), 25% ammonia solution (Merck), Potassium dihydrogen phosphate GR(Merck), Ammonium hepta molybdate tetrahydrate pure (Merck), Ammonium metaVanadate (LC, LOBA-Chemie, IndoAustranal Co, INDIA), Sodium carbonate anhydrate GR (Merck), Sodium chloride (Merck), Potassium nitrate purified (Merck), Sodium sulphate dry purified (Merck) and Conc. HNO_3 (Merck). All other chemicals used were of AR/GR grade.

2.2. Instruments

The phosphate solution containing adsorbent (AIR) was centrifuged at 5000 rpm (Refrigerated centrifuge RC 4100D, Eltek) at 30^0C. The absorbance of the Phosphate solution was measured spectrophotometer (Model: 104, Systronics) at λmax: 465 nm. P^H of the solution mixture before and after was measured by Digital pH meter (Model: 335, Systronics). X-ray diffraction (XRD) study of waste IOT and AIR were carried out at room temperature (Miniflex, Rigaku Corporation, Japan) at scanning rate of 0.05^0/sec over the range of $2\Theta = 10\text{-}70^0$. FT-IR spectra of the AIR contain phosphate materials were taken by Nicolet (Impact 410, Madison) FT-IR spectrometer by using KBr pellets. 2.3. Preparation of AIR from waste IOT

AIR sample was used in this study, obtained from waste IOT collected from Joda-Barbil industrial streets, Orissa, India. Known quantity around 20g of waste IOT was subjected to 1:1 HCl digestion at 80^0 C for 2 h. After cooling, it was filtered to separate the AIR with minimum washing using distilled water. Then it was dried at oven and then grinds with motorpastle. The AIR act as an adsorbent for the adsorptive removal of phosphate from contaminated water. The detail chemical analysis of waste IOT and AIR were given in our published journals [18,19].

2.4. Adsorption studies

A standard phosphate stock solution (1000mg/L) was prepared by dissolving an appropriate amount of analytical grade anhydrous KH_2PO_4 (Merck) in distilled water. Intermediate standard solutions (100mg/L) were prepared by standard solution were used in obtaining desired phosphate concentrations. Similarly, Carbonate, chloride, sulphate and nitrate standard solution were prepared from Na_2CO_3, NaCl, Na_2SO_4 and KNO_3 salt respectively in distilled water.

Adsorption of phosphate was carried out at ambient temperature in a Batch processes by varying contact time, pH of medium, adsorbate concentration, adsorbent dose and temperature. The whole process is carried out at pH ~ 6 gives maximum adsorption of phosphate. Accurately weighed sample of AIR (derived from waste IOT) was mixed with 50 ml phosphate solution of known concentration in a 100 ml conical flask with stopper was shaken in the water bath of a thermostat at a particular temperature for 2 h. In all cases, adsorption equilibrium was attained within ~ 2 h, and the pH ~ 6 was adjusted by adding a few drops of 0.1N NaOH or 0.1N HCl before shaking. The mixture was allowed to settle and was centrifuged at 5000 rpm for 5 min. The phosphate concentration in the supernatant was determined with a spectrophotometer (Model: 104, Systronics).

The amount of phosphate adsorbed per unit weight of AIR at time t, q_t (mg/g) and percentage of phosphate removal efficiency, R are calculated as follows:

$$q_t = (C_o - C_t)\, V / M \quad (1)$$

$$R = (C_o - C_t)\, 100 / C_o \quad (2)$$

where, C_o is the initial phosphate concentration (mg/L), C_t is the concentration of phosphate at any time t, V is the volume of solution (L) and M is the mass of AIR.

Inorder to study the adsorption isotherm, 0.2 g of AIR is kept in contact with 50 ml phosphate solution of different concentration (5, 10, 15, 20, 25, 30, 40, and 50 ppm) at pH ~ 6 for 2 h (to conform that equilibrium had been reached) with constant shaking at room temperature 30.2^0 C. After 2 h the solution attained equilibrium and the amount of phosphate adsorbed (mg/g) on the surface of adsorbent was determined by the difference of the two concentrations. Duplicate experiments are carried out for all the operating variables studied and only the average deviation of duplicate results in the units of concentration is found to vary as ± 2%. Blank experiments are carried out with phosphate solution and without adsorbent to ensure that no phosphate is adsorbed onto the wall of the beaker.

2.5. Adsorption isotherms

The Langmuir and Freundlich models are the simplest and most commonly used isotherms to represent the adsorption of component from liquid phase onto a solid phase[20]. The Langmuir model assumes monolayer adsorption while Freundlich model is empirical in nature which assumes the adsorption on heterogeneous surface. The adsorption data from the experiments were fitted to linearly transformed Langmuir and Freundlich equation. The Langmuir equation may be expressed as

$$C_{eq}/(x/m) = 1/(bX_m) + C_{eq}/X_m \quad (3)$$

where 'C_{eq}' is the equilibrium adsorbate concentration in solution, 'X_m' denotes the amount adsorbed to form monolayer (adsorption capacity), (x/m) is the amount adsorbed per unit mass of adsorbent, and 'b' is the binding energy constant. The Freundlich equation may be expressed as

$$\text{Log } (x/m) = 1/n \ (\log C_{eq}) + \log K \quad (4)$$

where K and 1/n are constants and considered to be relative indicators of adsorption capacity and adsorption intensity, respectively. The constants were obtained from the plots of the linearized equations. Another factor, R_L, which is considered as a more reliable indicator of adsorption [21-23] was computed from

$$R_L = 1/ (1 + bC) \quad (5)$$

where 'b' is Langmuir's constant and C is any adsorbate concentration at which the adsorption is carried out. Favorable adsorption is indicated by $0 < R_L < 1$.

2.6. Thermodynamic parameters

The thermodynamic parameters of the adsorption process are obtained from experimental at various temperatures using the following equations [24].

a) $\text{Log } K_d = \Delta S^0/(2.303R) - \Delta H^0/(2.303RT)$ (6)

b) $\Delta G^0 = \Delta H^0 - T\Delta S^0$ (7)

c) $K_d = (x/m)/ C_{eq}$ (8)

where K_d is the distribution coefficient for the adsorptive and is equal to the ratio of the amount of phosphate adsorbed (x/m, in mg/g) to the adsorptive concentration (C_{eq}, in mg/L) and T is the temperature in Kelvin. The values of ΔH^0 and ΔS^0 were determined from the slope and intercept of the linear plot of $\log K_d$ versus 1/T, from Eq. (6). Once these two parameters are obtained, ΔG^0 is determined from Eq. (7).

II. RESULTS AND DISCUSSION

3.1. Synthesis And Characterization Of AIR

AIR was synthesized from waste IOT as the starting materials in this study. The waste IOT have been subjected to 1:1 HCl digestion on a hot plate to extract the entire amount of Fe_2O_3 as $FeCl_3$. The AIR was removed by filtration, with minimum washing using distilled water. Then it was oven dried at 100^0C for 1h. Then it was used as adsorbent for adsorption of phosphate from contaminated water. The X-ray diffraction pattern of AIR is matched with the JCPDS database file(PDF-01-089-6538) which indicates that the AIR used in our work is ideal Kaolinite [$Al_2Si_2O_5(OH)_4$] with anorthic (triclinic) lattice structure [18,19]. Detail chemical analysis and the specific surface area of the AIR determined from BET surface analyzer is 119 m^2/g is described in our published journal [19].

3.2. Point Of Zero Net Proton Charge (P.Z.N.P.C.) For AIR

Potentiometric acid-base titration over the range of pH from 3 to 12 used to characterize the pH-dependent charge development on the amphoteric surface sites of AIR. Acid–base properties of AIR as ideal Kaolinite are attributed to protonation and deprotonation of the alumino functional group (≡Al-OH) on the edge; deprotonation of the silanol group (≡Si-OH) on the edge; and protonastion and deprotonation of doubly Co-ordinated based plane hydroxyl groups (≡Al_2-OH) (Ganor et al., 2003). The doubly co-ordinated basal plane hydroxyl group is less reactive than the aluminol group on the edge as such much of acid-base and adsorption reactions on kaolinite take place on the particle edge. The value of the p.z.n.p.c. of AIR used fro the adsorption experiment was determined by using procedure given by [19].

Reported p.z.n.p.c. values for other kaolinite samples range from 3.0 to 7.5 [24-27]. Some of the disagreement in the reported values can be attributed to differences in sample separation and to use of different models to interpret data. Detailed discussions on determination of p.z.n.p.c. values fro clay samples were presented elsewhere [28,29]. The estimated p.z.n.p.c. value of 5.8 for AIR is with in the range of values reported in literature for other kaolinite samples. As per definition, edge surfaces of AIR attain a net positive charge above pH 5.8 and a net negative charge below the sample pH value. The amount of phosphate ions adsorbed owing to electrostatic constraints.

3.3. Adsorption studies

3.3.1. Effect of contact time

The variation in percentage removal of phosphate with contact time at different initial concentration ranging from 10, 30 and 50 mg/L is presented in Fig. 1. It may be observed from the figure that the maximum amount of phosphate adsorption taking place with in the contact time of 2 h and becomes gradual there after. This indicates that the rate of adsorption is very slow. Data has been taken up-to 6 h of operation which close to attain equilibrium. After that no significant change in the extent of adsorption is observed. For the initial concentration of upto 10mg/L, more than 40 % adsorption has been observed, where as for 50 mg/L, the percentage removal of phosphate is 20%. From the above observation, it is evident that for lower initial concentration of phosphate, the adsorption is much high. The percentage removal of phosphate decreases with increase in initial concentration and takes longer time to reach equilibrium because of the fact that with increase in phosphate concentration there will be increased competition for the active adsorption sites and the adsorption process will increasingly slowing down. This explains the more adsorption time for higher concentration.

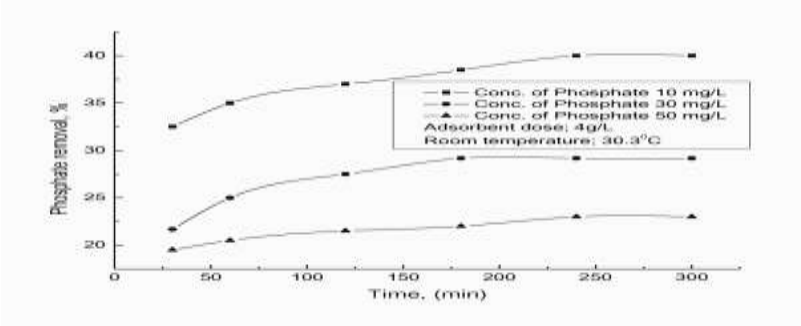

Fig. 1: Effect of contact time and initial concentration of Phosphate on the extent of adsorption.

3.3.2. Effect of pH

The pH of he medium is one of the important variables which significantly affects the extent of phosphate adsorption process particularly the adsorption capacity. pH of he solution may change: (1) the surface charge of the adsorbent, (2) the degree of ionization of the adsorbate molecule and (3) extent of dissociation of functional groups on the extent of phosphate, phosphate solution pH is varied from 3 to 12. The percentage of phosphate removal at different pH is shown in Fig. 2, for the initial phosphate concentration 10 mg/L. from this study, it is observed that maximum adsorption takes place at pH value of ≈ 7. Fig. 2. also shows that the removal of phosphate increases with increase of pH upto 7 and then it gradually decreases. The variation in phosphate uptake with respect to the initial solution pH can be explained on the basis of proton charge (p.z.n.p.c.) of AIR. For AIR the p.z.n.p.c. is estimated to be 5.8. Above this pH, the AIR particles acquire a negative surface charge leading to a lesser phosphate uptake. At a pH lower than p.z.n.p.c. the AIR surface acquires positive charge and phosphate become negative charge. Due to this there is an electrostatic attraction between phosphate molecules and AIR that causes increase in phosphate uptake.

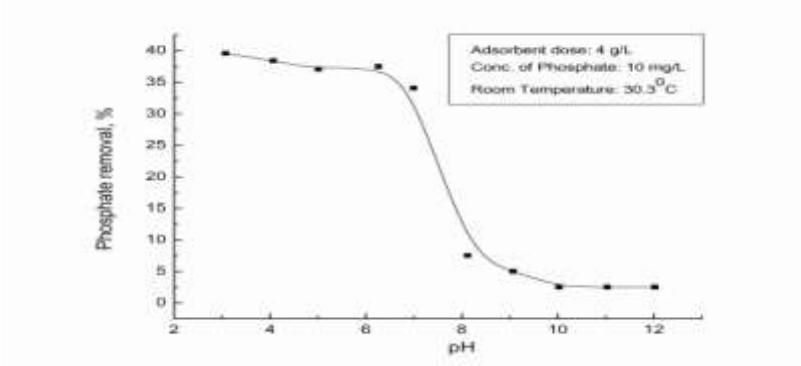

Fig. 2: Variation of pH of the phosphate solution with initial concentration of phosphate. Time of adsorption is 2 hr.

Earlier investigation also reported phosphate adsorption envelopes on kaolinite of a parabolic shape with phosphate adsorption maxima between pH 4 and 6 [28,29]. Development of adsorption envelopes for KGa-1 kaolinite is supported by the p.z.n.p.c_{edge}, value of 5.01 estimated by Scroth and Sposito, 1997. Abrupt changes

in electrostatic attraction between anions and the clay particle edge occur in the region of the p.z.n.p.c_{edge}, which translates in to changes in amount of phosphate ions adsorbed [6,8]. The silanol (≡SiOH) and aluminol (≡AlOH) functional groups located on the edge of AIR particles become deprotonated above the p.z.n.p.c_{edge}, resulting in developments of negative charges. Electrostatic repulsions are expected between the developed negative charge and the negatively charge phosphate ions, resulting in reduced adsorption of phosphate ions. Higher phosphate removal between pH 3 to 6 can be explained by inner sphere complexatiob of phosphate on the AIR surface via ligand exchange reaction mechanisms represented by Eq. (9) and (10) for monodentate and bidentate phosphate bonding respectively.

$$\equiv AlOH + H_2PO_4^- \leftrightarrow \equiv AlH_2PO_4 + OH^- \quad (9)$$

$$2 \equiv AlOH + H_2PO_4 \leftrightarrow (\equiv Al)_2HPO_4 + H_2O + OH^- \quad (10)$$

3.3.3. Effect Of Adsorbent Dose

Effect of AIR dose (varying from 4 to 10 g/L) on the phosphate uptake capacity at pH ~ 6, using an fixed initial phosphate concentration of 10 mg/L, and a run time of 2 h, was studied and the results are shown in Fig. 3. Initially, rapid increase in adsorption with the increase in adsorbent dose can be attributed to greater surface area and availability of more adsorption sites. After the critical dose (8 g/L) the extent of adsorption is increasingly slow down. It is observed from the figure (Fig. 3) that for the constant initial phosphate concentration, the phosphate uptake increases with increase in AIR dose. The slow down in phosphate uptake value (mg P/g of AIR) is due to the splitting effect of flux (concentration gradient) between adsorbate and adsorbent. Similar behavior has also been reported by M.W. Kamiyango et al., 2009 [30], that phosphate removal increased with 98.5% and 69.7% removal for TL-Ka and RL-Ka, respectively at a dose of 80 g/L. The maximum loading capacity is found to be 3.44 mg/g at an adsorbent dose of 4 g/L.

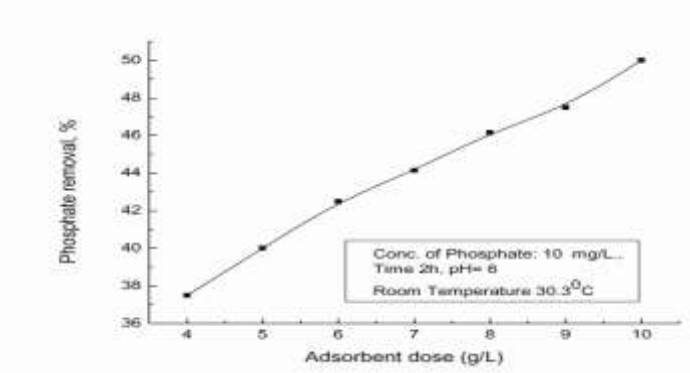

Fig. 3: Variation of phosphate adsorption with adsorbent dose. Time of adsorption is 2 hr.

3.3.4. Effect Of Initial Phosphate Concentration

The percentage of phosphate adsorbed at varying initial phosphate concentration (5mg/L to 50 mg/L) at pH ~ 6, using fixed adsorbent dose 4 g/L and a run time of 2 h, was studied and the results are shown in Fig. 4. It is observed from the Fig. 4 that for the constant adsorbent dose, the phosphate uptake decreases with increase in phosphate concentration. From the above observation, it is evident that for lower concentration of phosphate, phosphate uptake is higher. With increase in phosphate concentration, there will be increased competition for the active adsorption sites and the adsorption process will slow down. This explains lower adsorption occurs for higher phosphate concentration.

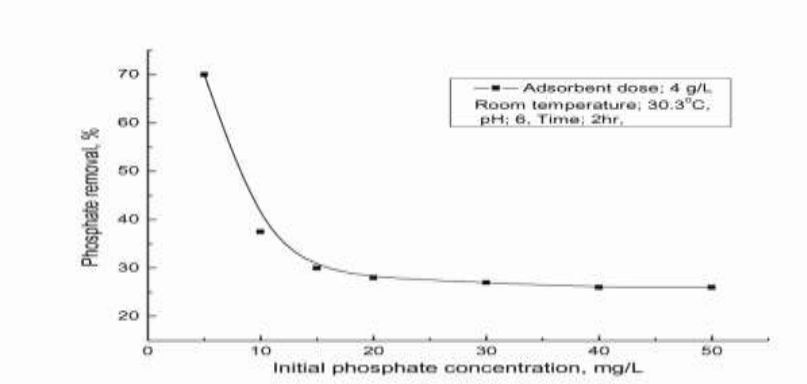

Fig. 4: Percentage removal of phosphate at varying initial phosphate concentration.

3.3.5. Effect of temperature.

To observe the effect of temperature on the adsorption capacity, experiments are carried out for five different phosphate concentrations (5, 10, 20, 30, 40, and 50 mg/L) and at three different temperature (30^0, 40^0, and 50^0 C) at pH ~ 6, using 4 g of AIR per liter of the solution. It has been observed that with increase in temperature, adsorption capacity increases as shown in Fig. 5. The thermodynamic parameters ΔG^0, ΔH^0 and ΔS^0 for the adsorption of phosphate been determined by using Eq. (6), (7) and (8). The values ΔG^0, ΔH^0 and ΔS^0 for the five different phosphate concentrations are shown in Table 1.

Table- 1 :Thermodynamic parameters for the adsorption of Phosphate at different temperatures.

Phosphate concentration (mg/L)	ΔH^0 (KJmol^{-1})	ΔS^0 (Jmol^{-1}K^{-1})	ΔG^0 (KJmol^{-1}) at different temperature		
			303.3 K	313 K	323K
10	3.282	1.10	330.01	341.01	352.01
30	11.15	1.74	516.1	533.49	550.89
50	36.01	3.80	1115.39	1153.39	1191.39

The adsorption is endothermic in nature since the value of ΔH^0 is positive. The endothermic nature is also indicated by increase in the amount of adsorption with temperature (Fig. 5). The adsorption is associated with increase in entropy which shows that the adsorbed phosphate molecules on the AIR surface are organized in more random fashion compared to those in the aqueous phase. Temperature affects not only precipitation of hydroxyapatite, but also the association/dissociation reactions of the related species and the thermodynamic solubility of hydroxyapatite [31]. The higher heat of adsorption obtained in this work indicates that chemisorptions rather than the physical adsorption are prevalent in this case.

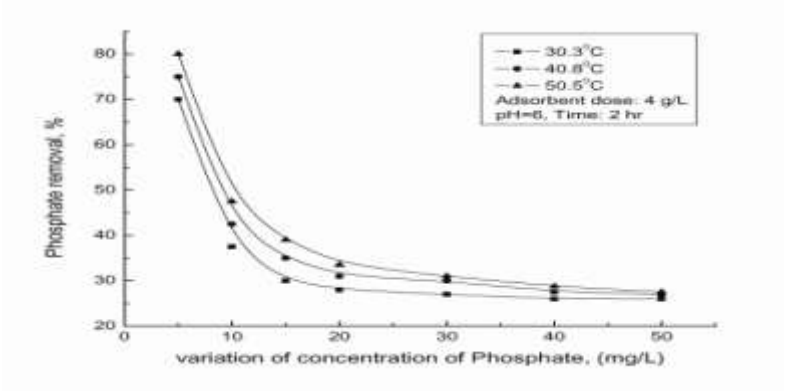

Fig. 5: Effect of temperature on the extent of adsorption at different phosphate concentration.

3.3.6. Effect of Co-existing anions.

Till now all the adsorption results discussed above were obtained taking phosphate ion only. However, in reality the phosphate contaminated water contains several other anions, which can equally complete in the adsorption process.

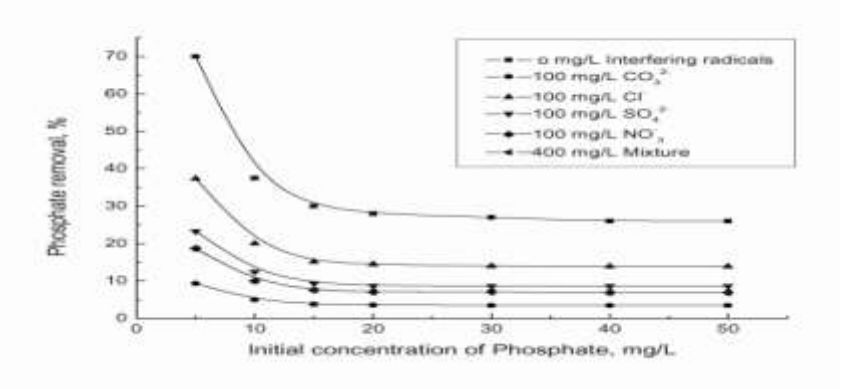

Fig. 6: Effect of co-existing ions with phosphate adsorption at different initial phosphate concentration.

In order to see effect of interfering ions an adsorption of phosphate, a mixture of known quantities commonly occurring anions in ground water, viz, sulphate (100 mg/L), chloride (100 mg/L), carbonate (100 mg/L), nitrate (100 mg/L) and mixture of all these ions (400 mg/L) were added into varying concentration of phosphate solution (5 to 50 mg/L) at pH~ 6, using fixed adsorbent dose (4g/L) and run time of 2 h. the dependence of such ions on adsorption of phosphate at varying initial concentration is shown in Fig. 6, phosphate uptake was decreased severely by chloride ions (55.55%) than sulphate ions (33.33%) than nitrate ions and mixture ions by (26.66%) and less affected by carbonate ions (13.33%). All the interfering radicals decrease the phosphate uptake on AIR from aqueous water.

3.3.7. Desorption studies

The basic assumption of desorption rate at any time would be proportional to the difference between the initial (at t = 0) amount of the adsorbed phosphate and the phosphate concentration in the solution, at any time t. Again, the phosphate concentration in the solution would be related to the amount of the phosphate still remaining adsorbed. The desorption of phosphate from loaded AIR by shaking with varying the pH from 7 to 12 for a predetermined optimal time period (2 h) is presented in Fig. 7. It is evident that there is practically no release of phosphate at lower pH and therefore quite safe for disposal at pH ≤ 7. However as pH increases the phosphate from loaded AIR get desorbed and nearly complete (~ 99 %) desorption of phosphate is obtained at pH ~ 11. thus phosphate gets reversibly adsorbed on the surface of AIR with in turn facilitates the recyclability of the material fro further use. Additional research warranted to optimize the exact regeneration conditions, assesses the loss of metals and adsorption efficiency after regeneration and determined of exact life cycles of AIR generated from waste IOT.

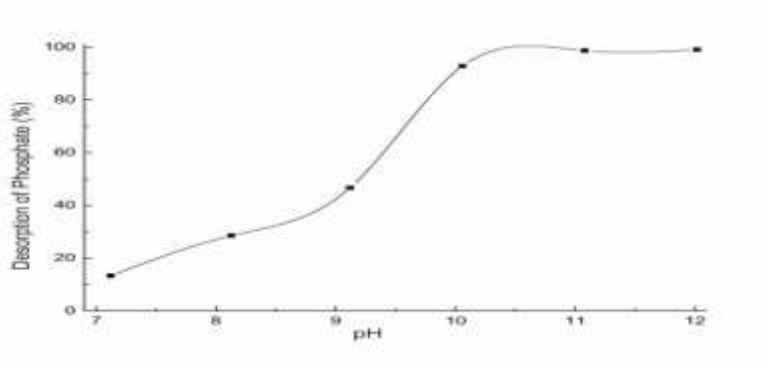

Fig. 7: Desorption studies of phosphate at variation of pH of the initial phosphate concentration.

3.3.8. Adsorption kinetics

In order to investigate the adsorption of phosphate on the surface of AIR, different kinetic models are used to examine the controlling mechanism of adsorption process. The proposed kinetic models are based on literature for sorption processes and adsorption capacity of adsorbent. In this study, pseudo-first order kinetic model, pseudo-second order kinetic model and intra-particle diffusion model are inve4stigated to find the best fitted model for the experimental data.

3.3.8.1. Pseudo-first order kinetic model

This model assumes that the rate of change of solute uptake with time is directly proportional to difference in saturation concentration and the amount of solid uptake with time. In most cases the adsorption reaction preceded by diffusion through a boundary, the kinetics follows the pseudo-first order rate equation. The rate constant of adsorption is expressed as a first-order rate expression given as [32].

$$dq_t/dt = K_t (q_e - q_t) \quad (11)$$

where q_t and q_e are the amount of phosphate adsorbed (mg/g) at contact time t (min) and at equilibrium, and K_t is the pseudo-first order rate constant(min^{-1}). After, integrating with the boundary conditions at initial time t =0, $q_t = 0$ and at any time (t>0), a mount of phosphate adsorbed is q_t and rearranging Eg. (11), the rate law for a pseudo-first order reaction becomes:

$$\log (q_e - q_t) = \log q_e - (k_1 / 2.303)\, t \quad (12)$$

The plot of log $(q_e - q_t)$ versus t (as shown in Fig. 8) should give a straight line with slope of - k_1 / 2.303 and intercept log q_e which allows calculation of adsorption rate constant k_1 and equilibrium adsorption capacity $q_{e.cal.}$ Calculated values of k_1 and $q_{e.cal}$ are summarized in Table 2. From Fig. 10 and q_e values (experimental and calculated) in Table 2, it may be concluded that the kinetics of phosphate adsorption on AIR is not probably following the pseudo-first order kinetic model and hence not a diffusion-controlled phenomena.

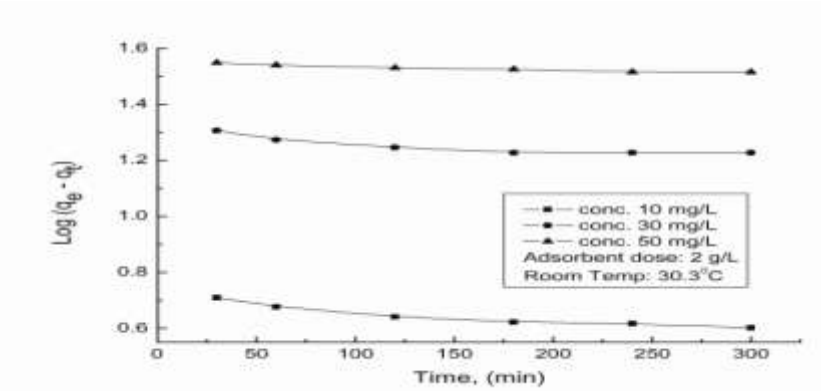

Fig. 8: Pseudo-first-order kinetic model for the adsorption of phosphate on AIR.

Table- 2: Pseudo-First-order and pseudo-Second-order kinetics model parameters for adsorption of phosphate on AIR at 303.3 K.

Initial Phosphate concentration (mg/L)	$q_{e,expt}$ (mg/g)	Pseudo-First-order kinetics			Pseudo-Second-order kinetics		
		$q_{e,cal}$ (mg/g)	K_1 (min^{-1})	R^2	$q_{e,cal}$ (mg/g)	K_1 (g/mg min)	R^2
10	2.00	5.050	9.17×10^{-4}	0.8863	2.0145	415.98×10^{-4}	0.9957
30	4.38	20.51	6.90×10^{-4}	0.9347	4.585	178.00×10^{-4}	0.9996
50	5.75	35.50	2.30×10^{-4}	0.9684	5.9066	162.95×10^{-4}	0.9993

3.3.8.2. Pseudo-second order kinetic model

Adsorption process with chemisorptions being the rate-control follows pseudo-second order model. The expression for pseudo-second order rate model is given as [32].

$$dq_t/dt = K_2 (q_e - q_t)^2 \quad (13)$$

where k_2 is the equilibrium rate constant for pseudo-second order reaction (g/mg min). Integration Eq. (13) using the boundary conditions at t =0 , q_t =0 and at any time t, amount of phosphate adsorbed is q_t and rearranging the rate law for a pseudo-second order reaction becomes:

$$t/q_t = 1/(k_2 q_e^2) + t/q_e \quad (14)$$

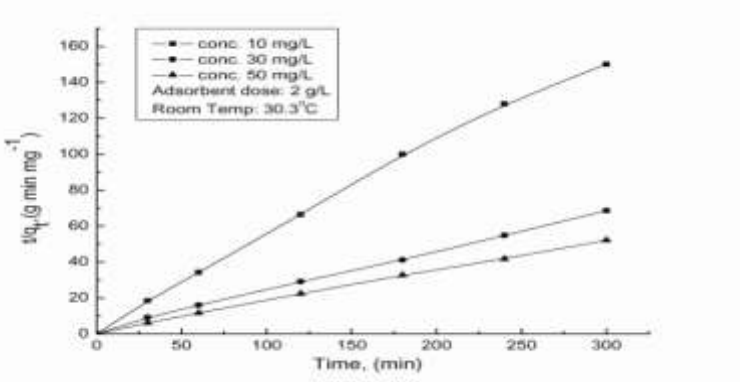

Fig. 9: Pseudo-second-order kinetic model for the adsorption of phosphate on AIR.

Fig. 9, shows that the plot of t/q_t versus t is a straight line with slope of $1/q_e$ and intercept $1/(k_2 q_e$. Using the value of q_e calculate from the slope, the value of k_2 is determined from the intercept. The calculated value of k_2, q_e and their corresponding regression coefficient (R^2) values are represented in Table 2. The value of regression coefficient is unity for 10 mg/Land nearly unity (≈ 0.99) for 30 and 40 mg/L of phosphate which

confirms that, the sorption kinetics of phosphate follows a pseudo-second order process. It may also be found from Table 3 that the calculate q_e values are very close to that of experimentally obtained q_e. Thus, it may be concluded that the adsorption of phosphate on AIR can be better explained by pseudo-second order kinetic model than that of first-order kinetic model and the process is chemisorptions controlled.

3.3.8.3. Intra-particle-diffusion model

In this model, it is assumed that the mechanism for phosphate removal by adsorption on sorbent material is taking place through four steps: (a) migration of phosphate molecules from bulk solution to the surface of the adsorbent through bulk diffusion, (b) diffusion of phosphate molecules through the boundary layer to the surface of the adsorbent via film diffusion; (c) the transport of the phosphate molecules from the surface to interior pores of the particle occur through intra-particle-diffusion or pore-diffusion mechanism and (d) the adsorption of phosphate at an active site on the surface of material by chemical reaction via ion-exchange, complexation and/or chelation. In general, the phosphate sorption is governed by either the liquid phase mass transport rate or through the intra-partcle mass transport rate. Pore-diffusion models should be formulated so as to consider not only the particles size but also particle shape. The importance of considering particle geometries (shapes and surfaces) in the formulation of pore-diffusion models is reported in the literature [33]. The potential effect of particle shape on the observed extent of adsorption is discussed in Ref. [34]. The adsorption process is a diffusive mass transfer process where the rate can be expressed in terms of the square root of time (t). The intra-particle-diffusion model is expressed as follows [35].

$$q_t = k_i t^{0.5} + I \qquad (15)$$

where q_t is the fraction dye uptake (mg/g) at time t, k_i is the intra-particle-doffusion rate constant (mg/(g $min^{0.5}$)) and I is the intercept (mg/g). the plot of q_t versus $t^{0.5}$ will give k_i as slope and I as intercept. The intercept I represents the effect of boundary layer thickness. Minimum is the intercept length, adsorption is less boundary layer controlled.

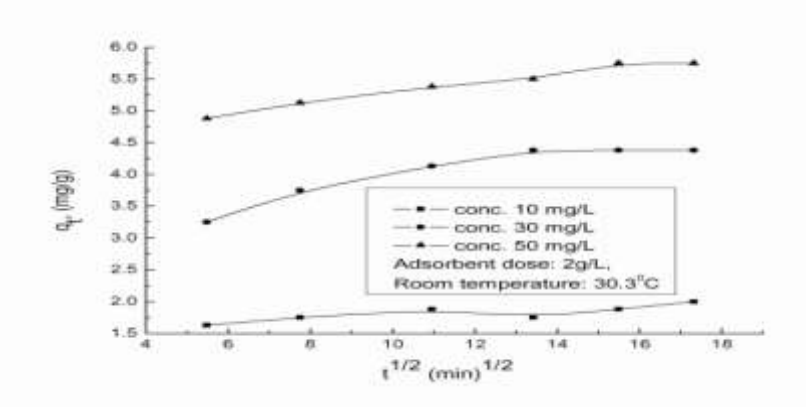

Fig. 10: Intra-particle-diffusion model for adsorption of phosphate onto AIR.

Fig. 10 represents the plot of q_t versus $t^{0.5}$ plot for the initial phosphate concentration 10, 30 and 50 mg/L. it seems that for all the three concentrations plots are nonlinear in nature but careful observation infer that data points can be better represented by double linear with difference in slope (k_i) and intercept (I).

Table: 3 Intra-particle-diffusion model for adsorption of phosphate on AIR at 303.3 K.

Initial Phosphate concentration (mg/L)	K_i, (mg/g $min^{1/2}$)	I (mg/g)	R^2
10	0.0269	1.5055	0.9424
30	0.1386	2.5747	0.9701
50	0.0714	4.5443	0.9823

The values of k_i and I are summarized in Table 3 along with regression constant (R^2) for differential phosphate concentrations. In first straight line, the sudden increase (with in a short time period) in slope signifies that the phosphate molecules are transported to the external surface of the AIR particles through film diffusion and its rate is very fast. After that, phosphate molecules are entered into the AIR particles by intraparticle-diffusion through pore, which is represented in second straight line. Both the line does not pass through the origin that concludes that both film diffusion and intra-particle-diffusion are simultaneously occurring during the adsorption of phosphate onto AIR.

3.3.9. Adsorption equilibrium

To determine the adsorption capacity of AIR obtained from waste IOT, equilibrium study has been performed to analyze the experimental data using well known Langmuir and Freundlich isotherm models at a room t4mperature 30.2 ^{0} C and at pH ~ 6. Adsorption properties and equilibrium parameters, commonly known as adsorption isotherms, describe how the adsorbate interacts with adsorbents, and comprehensive understanding of the nature of interaction. Isotherms help to provide information about the optimum use of adsorbents. So, in order to optimize the design of an adsorption system to remove phosphate from solutions, it is essential to establish the most appropriate correlation for the equilibrium curve. The Langmuir isotherm is based on the assumption that there is a finite number of binding sites which are homogeneously distributed over the adsorbent surface. These binding sites have the same affinity for adsorption of a single molecular layer and there is no interaction between adsorbent molecules. The basic assumption of his process is the formation of monolayer of adsorbate on the outer surface of adsorbent and after no further adsorption takes place [36]. The Langmuir isotherm is represented in Eq. (3).

The Freundlich isotherm model is an exponential equation that applies to adsorption on heterogeneous surfaces with interaction between adsorbed molecules and is not restricted to the formation of a monolayer. This model assumes that as the adsorbate concentration increases, the concentration of adsorbate on the adsorbent surface also increases and correspondingly that sorption energy exponentially decreases on complition of the sorption centers of an adsorbent. The well-known expression for the Freundlich model is given in Eq. (4).

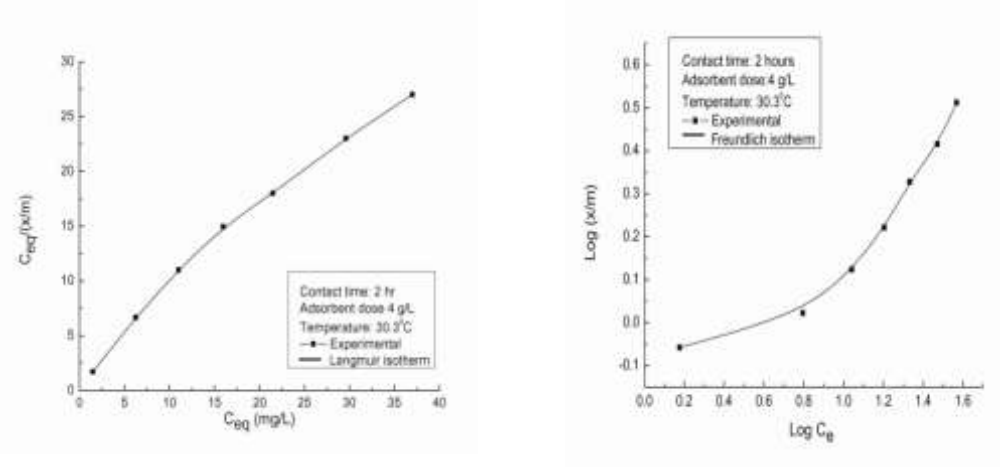

(a) (b)

Fig. 11: (a) Langmuir and (b) Freundlich adsorption isotherms for phosphate using AIR.

Table: 4: Adsorption constant for phosphate adsorption on AIR at room temperature (303.3 K)

Adsorbent	Freundlich constants			Langmuir constants			
	K	1/n	R^2	X_m (mg/g)	b (L/mg)	R^2	R_L
AIR (This work)	1.721	0.418	0.846	1.022	2.8084	0.999	0.007

The derived parameters from least square fittings of Langmuir and Freundlich equations were given in Table 4. From Fig. 11 and Table 4, it is evident that Langmuir model is slightly better fitted to the experimental

data (correlation coefficient ≥ 0.99). it may be noted that the derived monolayer adsorption capacities (X_m = 7.10 mg/g) for acid insoluble residue is slightly lower than the values reported for adsorption of phosphate on raw kaolin, pure kaolin , calcined raw kaolin and calcined pure kaolin [22].

III. CONCLUSION

This study shows that the AIR as an ideal kaolinite is an effective for the removal of phosphate from aqueous medium. The adsorption was highly dependent on various parameters, like: adsorbent dose, contact time, pH of the medium, initial phosphate concentration, temperature and co-existing ions. About 70% removal was observed for phosphate with in 2 h for 4 g/L AIR at 303 K. The percentage removal showed maxima at pH ~ 6. Adsorption process followed pseudo-second-order kinetics. The adsorption process was maximum in presence of temperature and endothermic in nature. However as pH increases the phosphate from loaded AIR get desorbed and nearly complete (~ 99 %) desorption of phosphate is obtained at pH ~ 11. thus phosphate gets reversibly adsorbed on the surface of AIR with in turn facilitates the recyclability of the material for further use.

REFERENCES

[1] H. Klapper, Control of Eutrophication in Inland water. Ellis Horwood, Chichester, 1991.
[2] Q. Zhou, C.E. Gibson, Y. Zhu, Chemosphere. 42 (2001) 221-225.
[3] M.J. Hammer, Jr. Hammer, Water and waste water Technology. Fourth ed. Prentice Hall, New jersey, USA, 2001.
[4] S.M.I. Sajidu, W.R.L. Masamba, E.M.T. Henry, S.M. Kuyeli, Water quality assessment in streams and waste water treatment plants of Blantyre. Malawi, Physics and Chemistry of the earth. 32 (2007)1391-1398.
[5] F.J. Hingston, A.M. Posner, J.P. Quirk, Discuss. Faraday. Soc. 52 (1971) 334.
[6] B.A. Manning, S. Goldberg, Soil. Sci. Soc. Am. J. 60 (1996) 121.
[7] A. Violante, M. Pigna, Soil. Sci. Soc. Am. J. 66 (2002) 1788.
[8] B.A. Manning, S. Goldberg, Modeling arsenate competitive adsorption on kaolinite, montmorillionite and illite. Clay. Clay. Miner. 44 (1996) 609-623.
[9] A.I. Omoike, G.W. Vanloon, Removal of phosphrous and organic matter removal by alum during waste water treatment. Water. Res. 33 (1999) 3617-3627.
[10] T. Clark, T. Stephenson, P.A. Dearse, Phosphorus removal by chemical precipation in a biological aerated filter, Water. Res. 31 (1997) 2557-2563.
[11] L. Ruixia, G. Jinlong, T.J. Hongxiao, Adsorption of fluoride, phosphate, and arsenate ions on a new type of ion exchange fiber. J. Collo. Inter. Sci. 248 (2002) 268-274.
[12] H.D. Stensel, Principles of biological phosphrous removal. In: Sedlak, R.I., Phosphorus and nitrogen removal from municipal waste water- principles and practice. Second ed., H.K. Lewis, London (1991) pp. 141.
[13] E.C. Moreno, K. Varughese, Crystal growth of calcium apatites from dilute solutions. J. Cryst. Growth. 53 (1981) 20-30.
[14] G.N. Anastassakis, K.K. Karageorgiou, M. Paschalis, Removal of phosphate species from solution by flotation, In: I. Gaballah, B. Mishra, R. Solozabal, M. Tanaka, (Eds). REWAS'04- Global symposium on recycling, Waste Treatment, Clean Technology, TMS-INASMET (2004) pp. 1147-1154.
[15] J.P. Boisvert, T.C. To, A. Berrak, C. Jolicoeur, Phosphate adsorption in flocculation process of aluminium sulphate and polyaluminiumsilicate-sulphate. Water. Res. 31 (1997) 1939-1946.
[16] K. Fytianos, E. Voudrias, N. Raikos, Modelling of phosphorus removal from aqueous and waste water samples using ferric ion. Environ. Pollut. 101 (1998) 123-130.
[17] S. Yeoman, T. Stephenson, J.N. Lester, R. Perry, The removal of phosphrous during waste water treatment. A Review, Environ. Pollut. 49 (1998) 183-233.
[18] S.K. Giri, N.N. Das, G.C. Pradhan, Synthesis and characterization of magnetite nanoparticles using waste iron ore tailings for adsorptive removal of dyes from aqueous solution, Colloids Surf., A 389 (2011) 43–49.
[19] S.K. Giri, N.N. Das, G.C. Pradhan, Magnetite powder and kaolinite derived from waste iron ore tailings for environmental applications, Powder Technol. 214 (2011) 513–518.
[20] N. Das, P. Pattanaik, R. Das, Defluoridation of drinking water using activated titanium rich bauxite. J. Collo. Inter. Sci. 292 (2005) 1-10.
[21] T.H. Vermeulan, K.R. Hall, L.C. Egleton, A. Acrivos, Ind. Eng. Chem. Fundam. 5 (1966) 212-223.
[22] D. Ghosh, K.G. Bhattacharyya, Adsorption of methylene blue on kaolinite. Appl. Clay. Sci. 20 (2002) 295-300.
[23] I.F. McConvey, G. Mckay, Chem. Eng. Process. 19 (1985) 267-275.

[24] S.A. Khan, R. Rehman, M.A. Khan, Adsorption of Cr (III), Cr (VI) and Ag (I) on bentonite. Waste Mange. 15 (1995) 271-282.
[25] J. Ganor, J. Cama, V. Metz, Surface protonation data of kaolinite-reevolution based on dissolution experiments. J. Collo. Inter. Sci. 264 (2003) 67-75.
[26] B.K. Scroth, G. Sposito, Surface charge properties of kaolinite. Clays. Clays. Miner. 45 (1997) 85-91.
[27] E. Tombacz, M. Szekeres, Surface charge heterogeneity of kaolinite in aqueous suspension in comparison with montmorillonite. Appl. Clay. Sci. 34 (2006) 105-124.
[28] Y.S.R. Chen, J.N. Butter, W. Stumm, Adsorption of phosphate on alumina and kaolinite from dilute aqueous solution. J. Collo. Inter. Sci. 43 (1973) 421-436.
[29] J.K. Eldwald, D.C. Toensing, M.C.Y. Leuny, Phosphate adsorption reactions with clay minerals. Environ. Sci. Tech. 10 (1976) 485-490.
[30] M.W. Kamiyango, W.R.L. Masamba, S.M.J. Sajidu, E. Fabiano, Phosphate removal from aqueous solutions using kaolinite obtained from Linthipe, Malawi. Phys. Chem. Earth. 34 (2009) 850-856.
[31] Y. Sony, H.H. Hahn, E. Hoffmann, Effects of solution conditions on the precipitation of phosphate for recovery, A. Thermo. Evalu. Chemos. 48 (2002) 1029-1034.
[32] M.K. Purkait, D.S. Gusain, S. DasGupta, S. De, Adsorption behavior of chrysoidine dye on activated charcoal and its regeneration characteristics using different surfactants, Sep. Sci. Technol. 39 (2004) 2419-2440.
[33] D.M. Ruthven, K.F. Loughlin, The effect of crystallite shape and size distribution on diffusion measurements in molecular sieves. Chem. Eng. Sci. 26 (1971) 577-584.
[34] J.J. Pignatello, F.J. Ferrandino, L.Q. Huangm, Elution of aged and freshly added herbicides from a soil. Environ. Sci. Technol. 27 (1993) 1563-1571.
[35] W.J. Weberm Jr., J.C. Morriss, Kinetics of adsorption on carbon from solution. J. Sanit. Eng. Div. Am. Soc. Civil Eng. 89 (1963) 31-60.
[36] M. Ozacar, I.A. Sengil, Adsorption of reactive dyes on calcined alunite from aqueous dolutions. J. Hazard. Mater. B98 (2004) 211-224.